From Exciton Resonance to Frequency Mixing in GaAs Multiple Quantum Wells

Y. H. Ahn, J. S. Yahng, J. Y. Sohn, K. J. Yee, S. C. Hohng, J. C. Woo, and D. S. Kim*
Department of Physics, Seoul National University, Seoul 151-742, Korea

T. Meier and S. W. Koch
Fachbereich Physik und Wissenschaftliches Zentrum für Materialwissenschaften, Philipps-Universität Marburg, Renthof 5, D-35032 Marburg, Germany

Y. S. Lim
Department of Applied Physics, Konkuk University, Chungju, Chungbook 380-701, Korea

E. K. Kim
Korea Institute of Science and Technology, Cheongryang, Seoul 136-791, Korea
(Received 15 January 1999)

Frequency mixing ($2\omega_1 - \omega_2$) is demonstrated in femtosecond nondegenerate four-wave mixing (FWM) on GaAs multiple quantum wells using two synchronized, independently tunable lasers. The frequency mixing component in the spectrally resolved FWM coexists with the exciton resonance, and it dominates over the exciton component at high intensity and high detuning. This off-resonant component is present only for delays smaller than the temporal pulse width, whereas the resonant exciton component survives for longer delays. [S0031-9007(99)09078-X]

PACS numbers: 71.35.Cc, 42.50.Md, 42.65.Hw, 78.47.+p

Nonlinear optical spectroscopy has provided considerable understanding of the interaction of light with matter, especially in the direct band gap semiconductors and corresponding heterostructures. Four-wave mixing (FWM) has been performed as a powerful means to examine both coherent and incoherent optical response in semiconductors. Since the initial demonstration of the third-order nonlinear process in a wide range of crystalline materials by Maker and Terhune [1], nondegenerate FWM has been performed in the form of phase conjugation in many cases. For instance, the measurement of the fundamental relaxation parameters was achieved through the ultrahigh resolution frequency domain FWM [2,3]. In addition, nondegenerate FWM has strong implications on the future applications such as wavelength conversion for telecommunication systems [4,5].

In the meantime, the development of ultrafast pulsed lasers has provided a direct insight into the fundamental phenomena associated with the relaxation and transport dynamics [6]. Nevertheless, thus far femtosecond transient FWM has largely focused on the dynamics of the exciton resonance, both because the exciton plays a dominant role in the optical excitation [7] and because most femtosecond wave mixing has been performed with degenerate pulses. Only recently, some nondegenerate interactions have been reported in the femtosecond regime, including the partially nondegenerate FWM by Cundiff *et al.* [8] and two color FWM using synchronized, independently tunable lasers by Kim *et al.* [9].

In this Letter, we report on femtosecond nondegenerate FWM, providing valuable information about the fundamental nonlinear optical response in semiconductors. It is shown that, besides the resonant exciton contribution, an off-resonant frequency mixing component ($2\omega_1 - \omega_2$) is present in the FWM signal, which has been overlooked in the previous studies. It is demonstrated that this component dominates at high intensity. The geometry of the experimental setup is shown in Fig. 1 describing a three beam nondegenerate FWM configuration. The third pulse with frequency ω_1 is diffracted by the nondegenerate grating formed by the two pulses with different frequencies; ω_1 (dashed line) and ω_2 (dotted line). The direction $\mathbf{k}_3(\omega_1) + \mathbf{k}_2(\omega_1) - \mathbf{k}_1(\omega_2)$ is chosen in order to rule out the diffraction of ω_2 at $\tau_1 = \tau_2 = 0$ ps by the degenerate grating formed by the two beams at ω_1. We use two independently tunable, passively mode-locked Ti:sapphire lasers that are synchronized by a homemade electronic switch [9]. We also use a 10–20 fs Ti:sapphire laser and pick up two energies from the broad laser spectrum [10]. In both cases, the pulse widths are about 150 fs. The investigated sample is $GaAs/Al_{0.25}Ga_{0.75}As$ multiple quantum wells (well and barrier width of 100 Å), etched to admit transmission geometry, and the temperature was kept at 10 K.

In Fig. 2(a), we show spectrally resolved FWM (SR-FWM) data at $\tau_1 = \tau_2 = 0$ ps (solid line) when ω_1 (dashed line) is tuned at 10 meV below the band gap and ω_2 (dotted line) at the exciton resonance. The peak intensity of each pulse was about 10 MW/cm^2 (I_0). At first glance, the broad tail arising below the heavy-hole exciton (HH) appears to be a transient diffraction at ω_1, that is, the instantaneous diffraction of the laser pulse [9,11]. However, there is a tail in the SR-FWM extending somewhat beyond the spectrum of ω_1. A

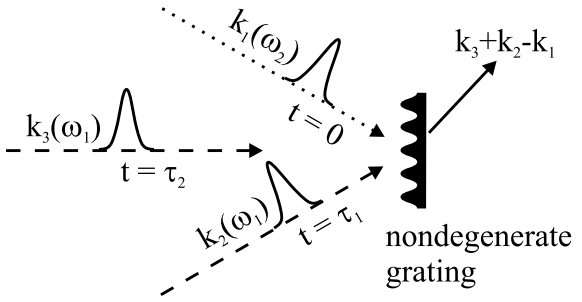

FIG. 1. The geometry of the experimental setup describing a three beam nondegenerate FWM configuration. The nondegenerate grating is formed by two pulses with ω_1 (dashed line) and ω_2 (dotted line), respectively, and diffracts the third pulse with frequency ω_1 to the phase matched direction $\mathbf{k}_3 + \mathbf{k}_2 - \mathbf{k}_1$. The investigated sample is $GaAs/Al_{0.25}Ga_{0.75}As$ multiple quantum wells (30 period, 100 Å).

resonant population grating is formed as long as spectral components of the off-resonant pump ω_1 overlap with HH that is coincident with the peak of ω_2, and, once formed, it decays with exciton lifetime. This population grating can diffract a wide range of spectra including off-resonant components, and we would expect the transient diffraction at ω_1 to decay with the exciton lifetime, just as the exciton resonance does. However, time-integrated FWM (TI-FWM) as a function of τ_2 shows a quite different result. Surprisingly, the TI-FWM signal at this tail (at 1.53 eV) decays with the pulse width, while at the exciton resonance (at 1.55 eV) it decays much slower, as shown in Fig. 2(b). The dip at the zero delay in the decay of the population grating is probably due to the interference between the third-order and higher-order processes contributing to the FWM signal [12,13]. Since the broad tail decays with the pulse width, it cannot originate from the transient diffraction of ω_1; instead, it is more plausible that another mechanism is involved in this phenomenon.

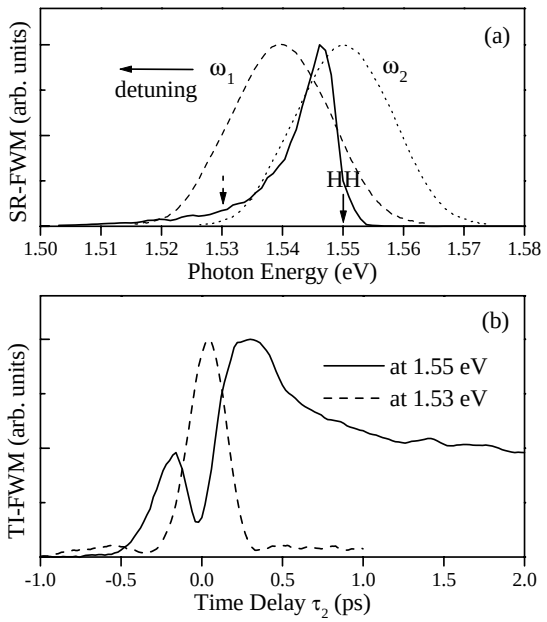

FIG. 2. (a) SR-FWM data at $\tau_1 = \tau_2 = 0$ (solid line) when ω_1 (dashed line) is tuned at 10 meV below the band gap and ω_2 (dotted line) at the exciton resonance ($I_0 \approx 10$ MW/cm^2). A broad tail arises below band gap, extending somewhat beyond the spectrum of ω_1. (b) TI-FWM as a function of τ_2 both at the tail (at 1.53 eV) and at the exciton resonance (at 1.55 eV) in the SR-FWM.

To unravel the mechanism responsible for this interesting phenomenon, we further increase the detuning of ω_1 as shown in Fig. 3(a). SR-FWM is shown at the zero time delay ($\tau_1 = \tau_2 = 0$ ps) for relatively high intensity ($5I_0 \approx 50$ MW/cm^2), when the center frequency of ω_1 is at 20 meV below HH and that of ω_2 (top). Surprisingly, another peak appears that is completely separated from the exciton and the pulse spectra. This pronounced peak is broader than the pulse spectrum and has its peak position exactly at $2\omega_1 - \omega_2$, which corresponds to that of the "frequency mixing" of the three pulses incident on the sample. The signal at $2\omega_1 - \omega_2$ disappears for time delays longer than the pulse width so that the exciton resonance completely dominates the FWM at $\tau_2 =$ 1 ps (bottom). This novel signal, temporally assigned to the frequency mixing, has not been reported before in

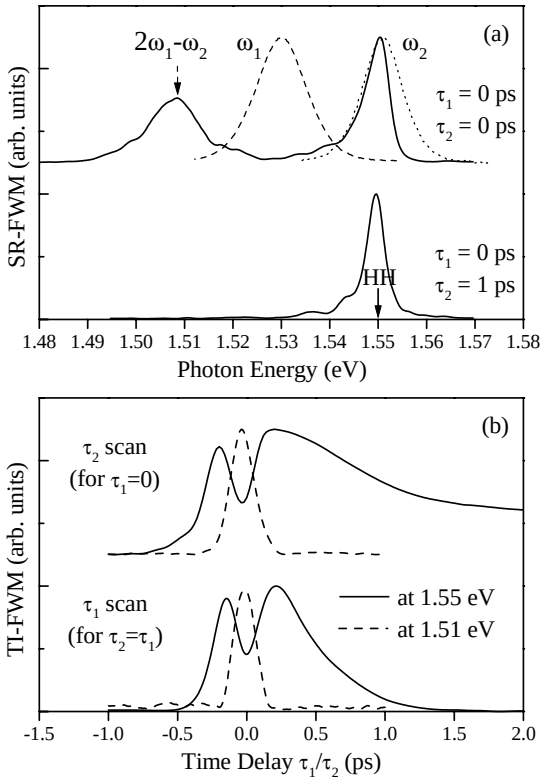

FIG. 3. (a) SR-FWM for relatively high intensity (50 MW/cm^2), when the center frequency of ω_1 is at 20 meV below the band gap and that of ω_2 at the exciton resonance for both $\tau_2 = 0$ ps (top) and $\tau_2 = 1$ ps (bottom). (b) TI-FWM as a function of both τ_2 for fixed $\tau_1 = 0$ (top) and τ_1 for $\tau_2 = \tau_1$ (bottom).

femtosecond coherent wave mixing. In addition, it is quite exciting that the frequency mixing is observed together with the exciton resonance in the coherent regime. Now we are interested in the condition for the transition from the exciton resonance to the frequency mixing as a function of intensity, time delay, detuning and so on.

Whereas in Fig. 3(a) the frequency mixing and the exciton components coexist, we find that at even higher intensities the frequency mixing completely dominates the SR-FWM (not shown in the figure). This is due to the fact that in our experimental condition the frequency mixing still increases rapidly with intensity. In contrast, the signal at the exciton resonance already is close to saturation and increases only gradually with the laser power.

The temporal evolution of the frequency mixing is displayed in more detail in Fig. 3(b). TI-FWM as a function of delay τ_2 permits a direct comparison between the frequency mixing and the exciton resonance as shown at the top of Fig. 3(b). As in the wide tail in Fig. 2(a), the frequency mixing decays with the pulse width, while the exciton component decays much slower with a time constant that is comparable to the exciton lifetime. Consequently, we can observe the transition between the two components by changing the time delay τ_2 as shown in Fig. 3(a). Note that while the exciton FWM signal peaks at about 200 fs, the frequency mixing signal has its maximum exactly at the zero delay. Therefore, the frequency mixing is not directly correlated with the dynamics of the exciton population.

Since the frequency mixing appears limited by the pulse width as a function of τ_2, the question arises whether it is in nature limited by the temporal overlap between the pulses or whether the short dephasing time at high intensity makes it appear so. At the bottom of Fig. 3(b), TI-FWM is plotted as a function of τ_1 for $\tau_2 = \tau_1$, which is analogous to the TI-FWM in the two beam self-diffraction geometry. It is clear that the $2\omega_1 - \omega_2$ decays with the pulse width as a function of the delay τ_1, whereas the exciton decays with a longer dephasing time. In other words, temporal overlap of the short pulses is indeed the dominant factor for the time domain frequency mixing, whereas the temporal evolution of the exciton coherence is determined by slower dephasing processes.

Finally, the SR-FWM as a function of ω_1 is shown for $\tau_1 = \tau_2 = 0$ in Fig. 4(a). The peak of the frequency mixing appears exactly at $2\omega_1 - \omega_2$ for every ω_1, the width of which is broader than that of the laser pulses, providing an indisputable evidence for the frequency mixing. In addition, a dramatic transition from the exciton resonance to the frequency mixing occurs, as ω_1 is moved further off resonance. Although the intensities of both components decrease with the increasing detuning, the resonant exciton component decreases much more severely for detunings higher than 10 meV, since spectral overlap is essential for a large exciton signal [8]. The frequency mixing also appears when ω_1 is tuned above

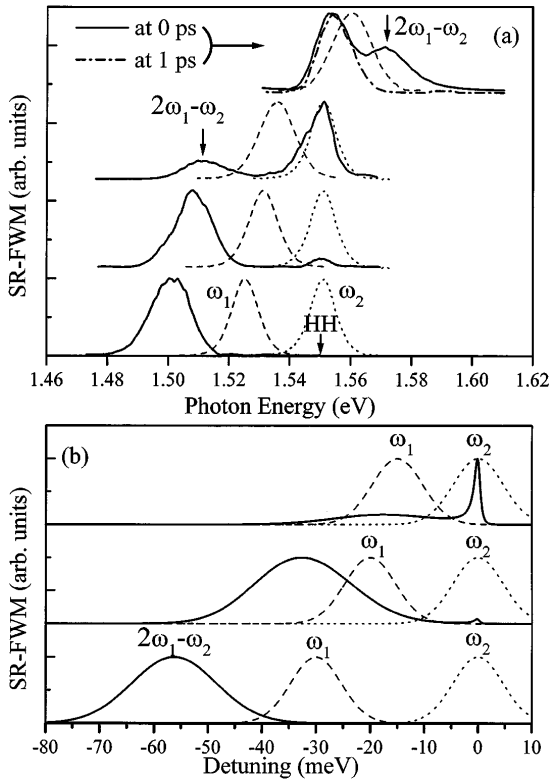

FIG. 4. (a) SR-FWM at the zero delay as a function of ω_1 for both below (bottom three, $10I_0$) and above (top, $20I_0$) the band gap. The peak of the frequency mixing appears exactly at that of $2\omega_1 - \omega_2$ for every ω_1, which is broader than that of the laser pulse. The frequency mixing for above the gap (solid line) is shown together with the data at $\tau_2 = 1$ ps (dash-dotted line). (b) Calculated SR-FWM at zero delay for various ω_1.

the exciton at higher intensity ($20I_0$) as shown at the top of Fig. 4(a). By analyzing the data at $\tau_2 = 1$ ps, it is clear that the high frequency component of the signal indeed vanishes and thus originates from the frequency mixing.

To qualitatively analyze our experimental findings, we have performed model calculations based on the semiconductor Bloch equations (SBE) [14] projected onto the 1 s HH exciton. In our third-order calculations of the nondegenerate FWM, an interband dephasing time of 1 ps was introduced phenomenologically. Figure 4(b) shows SR-FWM spectra calculated for $\tau_1 = \tau_2 = 0$ considering resonant ω_2 and various detunings of ω_1. For resonant excitation, the SR-FWM is peaked at the exciton and has a width which is determined by the homogeneous linewidth. With detuning of ω_1 to lower frequencies, tails toward lower frequencies appear in the SR-FWM. For large detuning, i.e., when the detuning is larger than the spectral pulse width, the broad frequency-mixed component at $2\omega_1 - \omega_2$ is clearly visible. In this regime, the resonant exciton component is negligible compared to the frequency-mixed component, demonstrating that the frequency mixing is existent already in third order. Although our theoretical model includes no microscopic

description of dephasing processes, it predicts that the frequency mixing component disappears if the delay between the pulses is longer than the temporal pulse width. This is due to the fact that for large positive delays the off-resonantly created grating has disappeared before the last pulse is incident on the sample. Thus, only the weak resonant component survives until the last pulse, and therefore the SR-FWM peaks at ω_1, i.e., at the frequency of the last pulse (not shown in the figure).

It is clear from Fig. 4 that the frequency mixing discussed so far corresponds to the phase conjugation that has been investigated extensively in incoherent wave mixing. To the best of our knowledge, in this Letter we report the first observation of the frequency mixing in the femtosecond coherent time domain on semiconductors, since so far most of the nondegenerate wave mixing experiments were performed on a nanosecond or longer time scale that is incoherent in nature. In other words, the frequency mixing observed here originates purely from the coherent interaction of the three pulses incident on the sample, allowing us to investigate its temporal evolution. In addition, unlike previous investigations of nondegenerate phase conjugation using two frequencies that are both resonant within the inhomogeneously broadened optical transition [2,3], the frequency mixing reported here involves completely off-resonant excitation (ω_1). It is also important to note here that the frequency mixing exists even when there is no spectral overlap between pulses [bottom of Fig. 4(a)], whereas it has been claimed that the spectral overlap might be essential in getting signals in the femtosecond coherent wave mixing [8]. In addition, it is clear that even in a situation with no spectral overlap between any of the three exciting pulses some nonlinear FWM signal, which may be extremely weak, exists.

The frequency mixing is not always resolved from the exciton, especially for lower intensities. Since the wide tail in Fig. 2(a) shows the same temporal profile as the frequency mixing, this tail can be attributed to the frequency mixing, although it is not clearly resolved from the exciton resonance in SR-FWM. This interpretation also provides a reasonable account for the broader spectrum compared to that of ω_1. Owing to the wide spectrum of femtosecond pulses, the frequency mixing might always induce contributions even to degenerate wave mixing at high intensities. The appearance of the frequency mixing, then, could be one of the causes for spectral broadening of the exciton resonance at high intensities observed in FWM.

In conclusion, we have demonstrated that nondegenerate femtosecond wave mixing in the coherent time domain gives rise to a novel signal component, that is, the frequency mixing, which has been investigated so far only in the incoherent time domain measurements. We prove that the frequency mixing readily appears at relatively high intensity even when it is not clearly resolved from the exciton resonance, for example, at lower intensity and at low detuning including degenerate wave mixing. From the unified viewpoint, we investigate the condition for the transition from the exciton resonance to the frequency mixing. We demonstrate that frequency mixing dominates at high intensity and high detuning and its existence is temporally limited by the pulse width, whereas the exciton is governed by the spectral pulse overlap and the dephasing time. The intensity of the frequency mixing is a very sensitive function of the intensity and the detuning, and further quantitative studies are necessary for a thorough understanding of this topic.

We were supported by the Lotte Foundation, the Korean Ministry of Education (1998–015-D00130), MOST (2N17300), and KOSEF (97-0702-03-01-3; 971-0209-037-2). The Marburg part of this work is supported by the Deutsche Forschungsgemeinschaft (DFG) through the Sonderforschungsbereich 383, the Quantenkohärenz Schwerpunkt, and the Leibniz program, and by the HLRZ Jülich through grants for extended CPU time on their supercomputer systems.

*Corresponding author.
Electronic address: denny@phya.snu.ac.kr

[1] P. D. Maker *et al.*, Phys. Rev. **137**, A801 (1965).
[2] U. Woggon *et al.*, Phys. Rev. B **51**, 4719 (1995).
[3] R. Tomasiunas *et al.*, Appl. Phys. Lett. **68**, 3296 (1996).
[4] J. Minch *et al.*, Appl. Phys. Lett. **70**, 1360 (1997).
[5] M. Tsuchiya *et al.*, Appl. Phys. Lett. **71**, 2650 (1997).
[6] J. Shah, *Ultrafast Spectroscopy of Semiconductors and Semiconductor Nanostructures* (Springer-Verlag, Berlin, 1996), and references therein.
[7] D. S. Kim *et al.*, Phys. Rev. Lett. **68**, 1006 (1992).
[8] S. T. Cundiff *et al.*, Phys. Rev. Lett. **77**, 1107 (1996).
[9] D. S. Kim *et al.*, Phys. Rev. Lett. **80**, 4803 (1998).
[10] P. Langot *et al.*, Opt. Commun. **137**, 285 (1997).
[11] D. S. Kim *et al.*, Phys. Rev. B **50**, 15 086 (1994).
[12] K. Leo *et al.*, Phys. Rev. Lett. **65**, 1340 (1990).
[13] M. Wegener *et al.*, Phys. Rev. A **42**, 5675 (1990).
[14] H. Haug and S. W. Koch, *Quantum Theory of the Optical and Electronic Properties of Semiconductors* (World Scientific, Singapore, 1994), 3rd ed.; M. Lindberg, R. Binder, and S. W. Koch, Phys. Rev. A **45**, 1865 (1992).